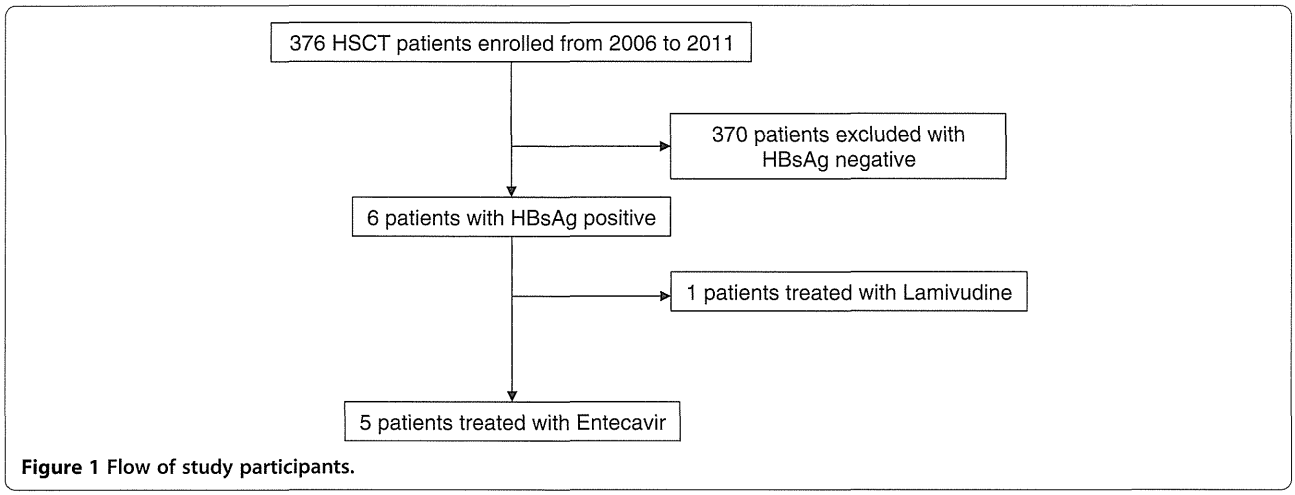

Figure 1 Flow of study participants.

HBV core and precore promotor mutations were not detected in all patients (Table 2).

ETV administration can prevent HBV flare and reactivation following HSCT.

The median observation period was 12.5 months (range, 2–50 months). ETV 0.5 mg once daily p.o. was administered as primary treatments for HBV infection. The ETV dose was increased after HSCT with patient #4 due to elevation of HBV viral load. Nevertheless all allogeneic-HSCT recipients suffered from mucous membrane disorder, no patient discontinue ETV oral administration. #4 and #5 patients developed renal disorder due to toxoplasmosis and adverse event of FK506 respectively. The ETV doses were reduced according to the kidney function in these patients. ETV was well tolerated in all cases and no patients discontinued ETV during the follow-up period for severe adverse events. There was no adverse drug interaction between ETV and other drugs. Median neutrophil engraftment time was 20 days (range 16–32 days) in allogeneic HSCT patients (#2-5). No cytopenia due to ETV treatment was observed in all patients. At the last follow-up, three patients (#1, #2 and #4) had died and the causes of mortality were aspergillus pneumonia, aggravation of underlying disease and toxoplasmosis, respectively.

In respect to immunosuppressive agent, two patients (#4 and #5) received mPSL 2 mg/kg i.v. in divided dose daily for acute GVHD in a short period. Patients #2 and #3 suffered chronic GVHD and continued to receive systemic steroid (mPSL 0.5 mg/kg and PSL 0.5 mg/kg i.v. in divided dose daily, respectively) and FK506 for the observation period. Patient #2 received a steroid pulse (mPSL 1000 mg i.v. in divided dose daily for 3 days) against exacerbation of chronic GVHD. Nevertheless, steroid treatment continued during GVHD in these patients and HBV DNA was not detected, indicating that ETV effectively protected against HBV flare and reactivation. In patients #3 and #4, MMF was also added for steroid-refractory GVHD.

There were no episodes of HBV flare or reactivation after HSCT in all patients during the observation period, as a 10-fold rise in HBV DNA levels or positive conversion of HBsAg were not observed. As shown in Figure 2, although patient #3 showed a significantly high HBV DNA level during the HSCT period, HBV flare was not observed. Serum HBsAg was not detected in patient #3

Table 1 Characteristics of 5 HSCT recipients treated with Entecavir

Case	Age (y)	Sex	Disease	Transplantation	GVHD prophylaxis	Steroid administration	cGVHD	Conditioning regimen	Observation period	Sstatus	Cause of death
#1	64	F	MM	Autologous	(–)	No	-	Mel	2 M	Dead	MM
#2	55	F	MDS-RAEB	Allogeneic	FK + MTX	Yes	Yes	BU + CY	9 M	Dead	Aspergillus Pneumonia
#3	24	F	MDS-RCMD	Allogeneic	FK + MTX	Yes	Yes	BU + CY	50 M	Alive	-
#4	58	F	AML	Allogeneic	CsA + MTX	Yes	No	BU + CY	4 M	Dead	Toxoplasmosis
#5	63	F	T-LBL	Allogeneic	FK + MTX	Yes	No	Flu + Mel + TBI(4Gy)	16 M	Alive	-

Abbreviation: MM multiple myeloma, *MDS* myelodysplastic syndrome, *RAEB* refractory anemia with excessive blast, *RCMD* refractory cytopenia with multilineage dysplasia, *AML* acute myeloid leukemia, *T-LBL* T lymphoblastic lymphoma, *FK* tacrolimus, *CsA* ciclosporin A, *Mel* melfalan, *BU* busulfan, *CY* cyclophosphamide, *TBI* total body irradiation, *Flu* fludarabine.

Aoki *et al. SpringerPlus* 2014, **3**:450
http://www.springerplus.com/content/3/1/450

Table 2 HBV markers of 5 HSCT recipients treated with Entecavir

Case	Genotype	HBsAg	HBsAb	HbcAb	BCP/Precore	Initial serum HBV DNA (xLog Copies/ml)	Flare after HSCT
#1	ND	(+)	(−)	(+)	ND	4	No
#2	C	(+)	(−)	(+)	ND	Undetectable	No
#3	B	(+)	(−)	(+)	Wild type	>7.6	No
#4	C	(+)	(−)	(+)	Wild type	Undetectable	No
#5	C	(+)	(−)	(+)	Wild type	7.4	No

Abbreviation: BPC basal core promoter, *ND* not determined.

at 18 months after the start of ETV. Subsequently, patient #3 showed reduction of HBV DNA to an undetectable level at the last follow-up.

Discussion and evaluation

A phase III trial reported that ETV has superior virological, histological and biochemical efficacy as an antiviral drug for HBV infection compared with LAM (Chang et al. 2006). Furthermore, ETV showed a low resistance rate compared with LAM (Tenney et al. 2009). Recent case reports have described successful treatment of HBV reactivation after HSCT with ETV (Christopeit et al. 2010; Milazzo et al. 2011). Therefore, ETV is a strong candidate as a substitute for LAM for HBV prophylaxis in HSCT.

The present study has shown the safety and efficacy of ETV treatment for protection against HBV flare after HSCT. Similar to previous reports for liver transplantation, (Fung et al. 2011) all the patients continued ETV through to the last follow-up without any intolerable adverse events. Intense immunosuppression during HSCT owing to the conditioning regimen and GVHD prophylaxis is a serious risk for HBV flare and reactivation. However, no HBV flare after HSCT was documented during our observation period with ETV treatment. Although blood count after HSCT is not stable, no cytopenia due to ETV was observed. Furthermore, no drug

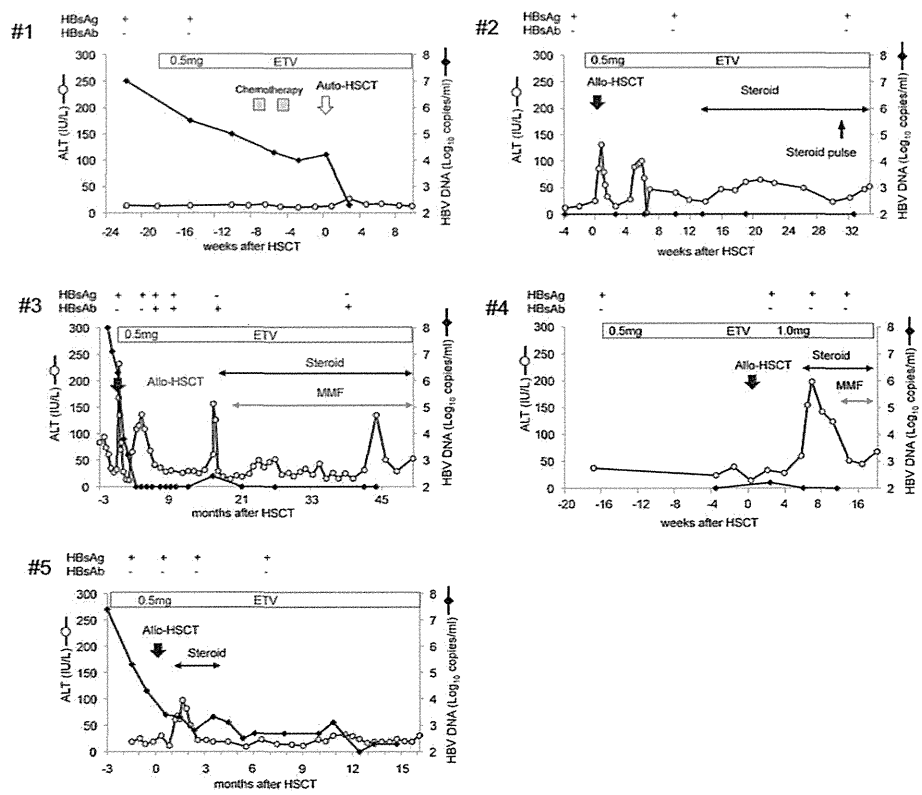

Figure 2 Clinical courses of HSCT patients treated with ETV. The X-axis shows the time course, and the Y-axes show the ALT levels and HBV DNA copy numbers, respectively. Transitions of HBsAg and HBsAb are shown at the top. No HBV DNA elevation was observed except for patient #3. HBV DNA of patient #3 became detectable level transiently. ALT elevation after HSCT was observed in all allogeneic HSCT recipients (#2-5). Causes of ALT elevation were considered GVHD or VOD.

interaction with ETV was documented after HSCT. Our study has demonstrated that ETV treatment is a promising candidate for HBV flare and reactivation prophylaxis in HSCT, similar to the case for liver transplantation.

Seroclearance of HBsAg and HBV DNA was observed with patient #3, despite a high HBV DNA level during the HSCT period. The timing of the serum HBsAg clearance was consistent with that in a liver transplantation study (Fung et al. 2011). Of the 5 patients tested, HBsAb was detectable with 1 patient (#3). The time of detection of HBsAb was 6 weeks after HSCT. HBsAb with patient #3 was detectable during the follow-up period. This positive conversion of HBsAb might be associated with HBsAg clearance (Fung et al. 2011).

All allogeneic HSCT patients showed serum ALT elevation after HSCT. Almost all cases showed ALT elevation without HBV DNA elevation or positive conversion of HBsAg, and we considered that these liver injuries were caused by GVHD or drug-induced hepatotoxicity. Serum ALT elevation and positive conversion of HBV DNA were observed at the same time with patient #3 at 17 months after the HSCT period. However, chronic GVHD symptoms, such as skin keratinization and oral dryness, were exacerbated around the same time and ALT decreased after systemic steroid and MMF administration. Moreover, the positive reaction for HBV DNA was transient and the presence of HBsAg conversely became negative. Collectively, based on these findings, we suggest that the ALT elevation might have been caused by chronic GVHD.

There are some limitations in this study, since it was retrospective and the number of patients was small. Half of the patients died within 1 year after HSCT and their observation periods were insufficient. In future, a large prospective study of ETV prophylaxis in HSCT is required.

Conclusions

In conclusion, our study showed that ETV monotherapy may be effective and safe after HSCT for patients with HBV. Our study will contribute to future clinical trials.

Competing interests

The authors declare that they have no competing interests.

Authors' contributions

K.K and H.S designed this study. J.A and K.K wrote the manuscript. J.A collected clinical information. K.K and K.O contributed the collection of clinical information. All authors read and approved the final manuscript.

Acknowledgements

We thank Dr. Masashi Mizokami for supporting this study.

Author details

[1]Hematology Division, Tokyo Metropolitan Cancer and Infectious Diseases Center Komagome Hospital, Tokyo, Japan. [2]Hepatology Division, Tokyo Metropolitan Cancer and Infectious Diseases Center Komagome Hospital, 3-18-22, Honkomagome, Bunkyo-ku, Tokyo 113-8677, Japan.

Received: 24 July 2014 Accepted: 6 August 2014
Published: 20 August 2014

References

Aritomi T, Yatsuhashi H, Fujino T, Yamasaki K, Inoue O, Koga M, Kato Y, Yano M (1998) Association of mutations in the core promoter and precore region of hepatitis virus with fulminant and severe acute hepatitis in Japan. J Gastroenterol Hepatol 13:1125–1132

Chang TT, Gish RG, de Man R, Gadano A, Sollano J, Chao YC, Lok AS, Han KH, Goodman Z, Zhu J, Cross A, DeHertogh D, Wilber R, Colonno R, Apelian D (2006) A comparison of entecavir and lamivudine for HBeAg-positive chronic hepatitis B. N Engl J Med 354:1001–1010

Christopeit M, Weber T, Abendroth J, Dollinger M, Lubbert C, Oehme A, Kekule AS, Behre G (2010) HBs seroconversion in a patient with acute hepatitis B treated with entecavir during immunosuppression against severe bronchiolitis obliterans in the course of chronic graft versus host disease. J Clin Virol 48:218–219

Fung J, Cheung C, Chan SC, Yuen MF, Chok KS, Sharr W, Dai WC, Chan AC, Cheung TT, Tsang S, Lam B, Lai CL, Lo CM (2011) Entecavir monotherapy is effective in suppressing hepatitis B virus after liver transplantation. Gastroenterology 141:1212–1219

Giaccone L, Festuccia M, Marengo A, Resta I, Sorasio R, Pittaluga F, Fiore F, Boccadoro M, Rizzetto M, Bruno B, Marzano A (2010) Hepatitis B virus reactivation and efficacy of prophylaxis with lamivudine in patients undergoing allogeneic stem cell transplantation. Biol Blood Marrow Transplant 16:809–817

Hammond SP, Borchelt AM, Ukomadu C, Ho VT, Baden LR, Marty FM (2009) Hepatitis B virus reactivation following allogeneic hematopoietic stem cell transplantation. Biol Blood Marrow Transplant 15:1049–1059

Hsiao LT, Chiou TJ, Liu JH, Chu CJ, Lin YC, Chao TC, Wang WS, Yen CC, Yang MH, Tzeng CH, Chen PM (2006) Extended lamivudine therapy against hepatitis B virus infection in hematopoietic stem cell transplant recipients. Biol Blood Marrow Transplant 12:84–94

Hui CK, Lie A, Au WY, Leung YH, Ma SY, Cheung WW, Zhang HY, Chim CS, Kwong YL, Liang R, Lau GK (2005) A long-term follow-up study on hepatitis B surface antigen-positive patients undergoing allogeneic hematopoietic stem cell transplantation. Blood 106:464–469

Knoll A, Boehm S, Hahn J, Holler E, Jilg W (2004) Reactivation of resolved hepatitis B virus infection after allogeneic haematopoietic stem cell transplantation. Bone Marrow Transplant 33:925–929

Lai CL, Rosmawati M, Lao J, Van Vlierberghe H, Anderson FH, Thomas N, Dehertogh D (2002) Entecavir is superior to lamivudine in reducing hepatitis B virus DNA in patients with chronic hepatitis B infection. Gastroenterology 123:1831–1838

Liang R, Lau GK, Kwong YL (1999) Chemotherapy and bone marrow transplantation for cancer patients who are also chronic hepatitis B carriers: a review of the problem. J Clin Oncol 17:394–398

Lo CM, Cheung ST, Lai CL, Liu CL, Ng IO, Yuen MF, Fan ST, Wong J (2001) Liver transplantation in Asian patients with chronic hepatitis B using lamivudine prophylaxis. Ann Surg 233:276–281

Milazzo L, Corbellino M, Foschi A, Micheli V, Dodero A, Mazzocchi A, Montefusco V, Zehender G, Antinori S (2012) Late onset of hepatitis B virus reactivation following hematopoietic stem cell transplantation: successful treatment with combined entecavir plus tenofovir therapy. Transpl Infect Dis 14(1):95–8

Mutimer D, Dusheiko G, Barrett C, Grellier L, Ahmed M, Anschuetz G, Burroughs A, Hubscher S, Dhillon AP, Rolles K, Elias E (2000) Lamivudine without HBIg for prevention of graft reinfection by hepatitis B: long-term follow-up. Transplantation 70:809–815

Orito E, Ichida T, Sakugawa H, Sata M, Horiike N, Hino K, Okita K, Okanoue T, Iino S, Tanaka E, Suzuki K, Watanabe H, Hige S, Mizokami M (2001) Geographic distribution of hepatitis B virus (HBV) genotype in patients with chronic HBV infection in Japan. Hepatology 34:590–594

Perrillo RP, Wright T, Rakela J, Levy G, Schiff E, Gish R, Martin P, Dienstag J, Adams P, Dickson R, Anschuetz G, Bell S, Condreay L, Brown N (2001) A multicenter United States-Canadian trial to assess lamivudine monotherapy before and after liver transplantation for chronic hepatitis B. Hepatology 33:424–432

Tenney DJ, Rose RE, Baldick CJ, Pokornowski KA, Eggers BJ, Fang J, Wichroski MJ, Xu D, Yang J, Wilber RB, Colonno RJ (2009) Long-term monitoring shows hepatitis B virus resistance to entecavir in nucleoside-naive patients is rare through 5 years of therapy. Hepatology 49:1503–1514

Tomblyn M, Chiller T, Einsele H, Gress R, Sepkowitz K, Storek J, Wingard JR, Young JA, Boeckh MJ (2009) Guidelines for preventing infectious complications among hematopoietic cell transplantation recipients: a global perspective. Biol Blood Marrow Transplant 15:1143–1238

Xi ZF, Xia Q, Zhang JJ, Chen XS, Han LZ, Wang X, Shen CH, Luo Y, Xin TY, Wang SY, Qiu de K (2009) The role of entecavir in preventing hepatitis B recurrence after liver transplantation. J Dig Dis 10:321–327

Xunrong L, Yan AW, Liang R, Lau GK (2001) Hepatitis B virus (HBV) reactivation after cytotoxic or immunosuppressive therapy–pathogenesis and management. Rev Med Virol 11:287–299

doi:10.1186/2193-1801-3-450
Cite this article as: Aoki *et al.*: Efficacy and tolerability of Entecavir for hepatitis B virus infection after hematopoietic stem cell transplantation. *SpringerPlus* 2014 **3**:450.

Hepatology Research

Hepatology Research 2014; 44: 173–175 doi: 10.1111/hepr.12158

Editorial

Should we try antiviral therapy for hepatitis C virus infection with pyoderma gangrenosum-like lesions?

See article in *Hepatology Research* 44: 238–245
Eradication of hepatitis C virus could improve immunological status and pyoderma gangrenosum-like lesions
Yasuteru Kondo, Tomoaki Iwata, Takahiro Haga, Osamu Kimura, Masashi Ninomiya, Eiji Kakazu, Takayuki Kogure, Tatsuki Morosawa, Setsuya Aiba and Tooru Shimosegawa

Pyoderma gangrenosum (PG) is a rare, ulcerative and painful neutrophilic dermatosis without any infectious signs. PG usually begins with pustules, red papules, plaques or nodules that rapidly grow to ulcerations with undetermined purple borders.[1] Five clinical variants have been characterized: classic, bullous, pustular, vegetative and peristomal types. Although PG is idiopathic in 25–50% of cases, approximately 50% of clinical cases are associated with underlying systemic diseases such as inflammatory bowel disease, rheumatological disease, paraproteinemia, hematological malignancies, and HIV and hepatitis virus infection.[2] PG may be due to neutrophilic dysfunction, autoinflammation, genetic factors and/or inflammatory cytokines.[3] PG is diagnosed by excluding other cutaneous ulcerative diseases by biopsy and identification of clinical features, because PG has no specific histopathological features. There is no gold standard for treatment of PG, therefore, therapy should focus on the associated underlying systemic disease. In addition to local wound management and pain control, topical or systemic agents have been considered. For mild and superficial lesions, topical agents (e.g. corticosteroids, tacrolimus and cyclosporin) are administrated. When more effective treatment is required, corticosteroids and cyclosporin are considered as first-line systemic agents. Recently, the use of tumor necrosis factor (TNF)-α inhibitors for PG has emerged, and infliximab is the only efficacious systemic agent.[4,5]

Hepatitis C virus (HCV) infection may present with various cutaneous manifestations such as urticaria, pruritus, cryoglobulinemia, erythema multiforme, granuloma annulare, porphyria cutanea tarda, vasculitis, lichen planus, vitiligo, erythema nodosum, pityriasis rubra pilaris and perniosis-like lesions.[6] PG is thought to be an extrahepatic cutaneous manifestation of HCV infection, although its frequency is low.[7] Only few cases of PG associated with chronic hepatitis C have been reported. Smith *et al.* reported the first case of chronic hepatitis C and PG.[8] Several skin biopsies were performed, but leukocytoclastic vasculitis in cutaneous ulcerative lesions on the lower legs, with typical clinical manifestations of PG, was not observed. Therefore, it was suggested that the PG-like lesion was not associated with mixed cryoglobulinemia (MC) because of the absence of histological findings. Treatment with interferon (IFN)-α-2a was started and the lesion improved within 5 weeks. Keane *et al.* reported another case, in which biopsies of ulcerative lesions in the lateral aspect of the calf showed a dense mixed lymphocytic infiltration in the dermis and vasculitis in the erythematous ulcer rim. Treatment with topical clobetasol and systemic minocycline resulted in improvement within several weeks, and there was no recurrence during 4 months of follow-up.[9] Currently, no specific treatment regimen for PG associated with chronic hepatitis C has been established, because there are few case reports and the pathogenic mechanism is still unknown.

In general, PG is also associated with the administration of drugs such as granulocyte colony-stimulating factor,[10] antipsychotic agents and IFN-α.[11] Indeed, IFN-α treatment has some well-known cutaneous side-effects such as dry skin, hair loss and vitiligo.[12,13] Furthermore, cutaneous ulcerations, indurated erythema and leukocytoclastic vasculitis may occur at IFN-α injection sites. The pathogenesis of local cutaneous reactions against IFN-α is still unknown. Several case reports have suggested that PG results from IFN-α treatment during the course of hematological malignancies. One case was improved by treatment with cyclosporin A and prednisone.[14] In addition, serum levels of TNF-α, interleukin

(IL)-6 and soluble IL-2 receptor increased when the cutaneous lesions appeared and returned to normal levels when the lesion healed. This indicated that the onset of PG was required for elevated inflammatory cytokine levels.[14] Furthermore, Yurci *et al.* reported the first PG case resulting from pegylated (PEG)-IFN-α-2a during the treatment of chronic hepatitis C.[15] Four weeks after starting PEG-IFN-α-2a treatment, cutaneous ulcerative lesions were clinically suspected as PG appeared, and treatment was discontinued after 8 weeks. After withdrawal of PEG-IFN-α-2a, PG-like lesions improved. Thus, PEG-IFN-α-2a may trigger cutaneous side-effects because pegylation allows stable serum levels of drugs.

Thus, the pathogenesis of PG with chronic hepatitis C is still unclear, suggesting that PG related to chronic hepatitis C is not associated with MC, but with other immunological mechanisms. In a study reported in this issue, Kondo *et al.* examined whether peripheral blood mononuclear cells (PBMC), including activated B cells, T-helper (Th)1 cells, Th2 cells, Th17 cells and $CD4^+CD25^+IL7R^-$ regulatory T cells (Treg) were involved in PG disease activity.[16] They demonstrated that Th17 cell numbers were markedly higher in patients with chronic hepatitis C and PG compared with those without extrahepatic immunological complications. In addition, after clearance of HCV following IFN therapy, the abnormal immunological status returned to normal and the PG-like lesions recovered without immunosuppressive therapy. These findings suggest that Th17 cells have an important role in the onset of PG, although it is still unknown whether these cells are HCV specific. As reported in this issue, HCV-infected CD4 T cells are required for disease progression, suggesting that HCV-specific Th17 cells are responsible for development of PG.

Th17 immunity has been identified during HCV infection, and PBMCs from HCV antibody positive patients secrete IL-17, IFN-γ, IL-10, and transforming growth factor (TGF)-β in response to stimulation with HCV non-structural protein (NS)4. The authors suggested that both HCV-specific Th1 and Th17 cells were suppressed by NS4-induced production of the innate anti-inflammatory cytokines, IL-10 and TGF-β.[17] This suggests that HCV infection suppresses antigen-specific Th17 cell functions and is responsible for induction of persistent chronic infection.

Although it has not been demonstrated that PG-like lesions are not associated with cryoglobulinemia, Kondo *et al.* have suggested an alternative hypothesis in which the pathogenesis of PG-like lesions with chronic hepatitis C is associated with Th17-related immunity. To the best of our knowledge, this report is the first evidence that the onset of PG is related to the number and cytokine production of Th17 cells.

According to the study reported in this issue and other recent reports, PG may be induced by IFN treatment as well as HCV infection. Kondo *et al.* have demonstrated that IFN treatment is more effective than immunosuppressants for the treatment of PG in the case of HCV infection. Thus, when a case presents with HCV and PG it may be useful to consider IFN treatment. The validity of IFN for PG should be verified by accumulating a greater number of clinical cases.

Kiminori Kimura
Hepatology Division, Tokyo Metropolitan Cancer and Infectious Diseases Center Komagome Hospital, Tokyo, Japan

REFERENCES

1 Wollina U, Haroske G. Pyoderma gangraenosum. *Curr Opin Rheumatol* 2011; **23**: 50–6.
2 Miller J, Yentzer BA, Clark A, Jorizzo JL, Feldman SR. Pyoderma gangrenosum: a review and update on new therapies. *J Am Acad Dermatol* 2010; **62**: 646–54.
3 Ruocco E, Sangiuliano S, Gravina AG, Miranda A, Nicoletti G. Pyoderma gangrenosum: an updated review. *J Eur Acad Dermatol Venereol* 2009; **23**: 1008–17.
4 Adisen E, Oztas M, Gurer MA. Treatment of idiopathic pyoderma gangrenosum with infliximab: induction dosing regimen or on-demand therapy? *Dermatology* 2008; **216**: 163–5.
5 Hughes AP, Jackson JM, Callen JP. Clinical features and treatment of peristomal pyoderma gangrenosum. *JAMA* 2000; **284**: 1546–8.
6 Mehta S, Levey JM, Bonkovsky HL. Extrahepatic manifestations of infection with hepatitis C virus. *Clin Liver Dis* 2001; **5**: 979–1008.
7 Crowson AN, Nuovo G, Ferri C, Magro CM. The dermatopathologic manifestations of hepatitis C infection: a clinical, histological, and molecular assessment of 35 cases. *Hum Pathol* 2003; **34**: 573–9.
8 Smith JB, Shenefelt PD, Soto O, Valeriano J. Pyoderma gangrenosum in a patient with cryoglobulinemia and hepatitis C successfully treated with interferon alfa. *J Am Acad Dermatol* 1996; **34**: 901–3.
9 Keane FM, MacFarlane CS, Munn SE, Higgins EM. Pyoderma gangrenosum and hepatitis C virus infection. *Br J Dermatol* 1998; **139**: 924–5.
10 Farina MC, Requena L, Domine M, Soriano ML, Estevez L, Barat A. Histopathology of cutaneous reaction to granulocyte colony-stimulating factor: another pseudomalignancy. *J Cutan Pathol* 1998; **25**: 559–62.

11 Mir-Bonafe JM, Blanco-Barrios S, Romo-Melgar A, Santos-Briz A, Fernandez-Lopez E. Photoletter to the editor: localized pyoderma gangrenosum after interferon-alpha2b injections. *J Dermatol Case Rep* 2012; **6**: 98–9.
12 Berk DR, Mallory SB, Keeffe EB, Ahmed A. Dermatologic disorders associated with chronic hepatitis C: effect of interferon therapy. *Clin Gastroenterol Hepatol* 2007; **5**: 142–51.
13 Hadziyannis SJ. Skin diseases associated with hepatitis C virus infection. *J Eur Acad Dermatol Venereol* 1998; **10**: 12–21.
14 Montoto S, Bosch F, Estrach T, Blade J, Nomdedeu B, Nontserrat E. Pyoderma gangrenosum triggered by alpha2b-interferon in a patient with chronic granulocytic leukemia. *Leuk Lymphoma* 1998; **30**: 199–202.
15 Yurci A, Guven K, Torun E *et al.* Pyoderma gangrenosum and exacerbation of psoriasis resulting from pegylated interferon alpha and ribavirin treatment of chronic hepatitis. C. *Eur J Gastroenterol Hepatol* 2007; **19**: 811–5.
16 Kondo Y, Iwata T, Haga T *et al.* Eradication of hepatitis C virus could improve immunological status and pyoderma gangrenosum-like lesions. *Hepatol Res* 2014; **44**: 238–45.
17 Lemmers A, Moreno C, Gustot T *et al.* The interleukin-17 pathway is involved in human alcoholic liver disease. *Hepatology* 2009; **49**: 646–57.

Hara et al. SpringerPlus 2014, 3:221
http://www.springerplus.com/content/3/1/221

SpringerPlus
a SpringerOpen Journal

RESEARCH Open Access

LAP degradation product reflects plasma kallikrein-dependent TGF-β activation in patients with hepatic fibrosis

Mitsuko Hara[1], Akiko Kirita[1], Wakako Kondo[1], Tomokazu Matsuura[2], Keisuke Nagatsuma[3], Naoshi Dohmae[4], Shinji Ogawa[5], Shinobu Imajoh-Ohmi[6], Scott L Friedman[7], Daniel B Rifkin[8] and Soichi Kojima[1*]

Abstract

Byproducts of cytokine activation are sometimes useful as surrogate biomarkers for monitoring cytokine generation in patients. Transforming growth factor (TGF)-β plays a pivotal role in pathogenesis of hepatic fibrosis. TGF-β is produced as part of an inactive latent complex, in which the cytokine is trapped by its propeptide, the latency-associated protein (LAP). Therefore, to exert its biological activity, TGF-β must be released from the latent complex. Several proteases activate latent TGF-β by cutting LAP. We previously reported that Camostat Mesilate, a broad spectrum protease inhibitor, which is especially potent at inhibiting plasma kallikrein (PLK), prevented liver fibrosis in the porcine serum-induced liver fibrosis model in rats. We suggested that PLK may work as an activator of latent TGF-β during the pathogenesis of liver diseases in the animal models. However, it remained to be elucidated whether this activation mechanism also functions in fibrotic liver in patients.

Here, we report that PLK cleaves LAP between R^{58} and L^{59} residues. We have produced monoclonal antibodies against two degradation products of LAP (LAP-DP) by PLK, and we have used these specific antibodies to immunostain LAP-DP in liver tissues from both fibrotic animals and patients.

The N-terminal side LAP-DP ending at R^{58} (R^{58} LAP-DP) was detected in liver tissues, while the C-terminal side LAP-DP beginning at L^{59} (L^{59} LAP-DP) was not detectable. The R^{58} LAP-DP was seen mostly in α-smooth muscle actin-positive activated stellate cells.

These data suggest for the first time that the occurrence of a PLK-dependent TGF-β activation reaction in patients and indicates that the LAP-DP may be useful as a surrogate marker reflecting PLK-dependent TGF-β activation in fibrotic liver both in animal models and in patients.

Keywords: Biomarker; Hepatic stellate cells; Liver fibrosis; Plasma kallikrein (PLK); TGF-β activation

Background

Liver fibrosis is characterized as the pathological deposition of excessive extracellular matrix (ECM), which finally causes hepatic dysfunction (Bataller and Brenner 2005). A key driver of fibrosis is the 25 kD homodimeric cytokine, transforming growth factor (TGF)-β (Dooley and ten Dijke 2012). TGF-β is produced as a latent complex; therefore, an essential step for controlling TGF-β activity is its activation, a process in which biologically active TGF-β is released from the latent complex (Figure 1a) (Dabovic and Rifkin 2008).

TGF-β1 is produced as a 390 amino acid precursor protein consisting of a signal peptide of 29 amino acids, an N-terminal pro-region called latency-associated protein (LAP), and a C-terminal region that becomes the active TGF-β1 molecule, and each region dimerized through S-S bonds. After processing by cleavage at R^{278}-A^{279} by a furin-like protease, the LAP non-covalently binds the mature TGF-β1, forming small latent complex (SLC) and preventing active TGF-β1 from binding its cognate receptors (Figure 1a). The active TGF-β1 and the LAP homodimer are 25 kD and 75 kD, respectively. The SLC is S-S bonded to another gene product, the latent

* Correspondence: skojima@riken.jp
[1]Micro-signaling Regulation Technology Unit, RIKEN Center for Life Science Technologies, 2-1 Hirosawa, Wako, Saitama 351-0918, Japan
Full list of author information is available at the end of the article

Hara et al. SpringerPlus 2014, 3:221
http://www.springerplus.com/content/3/1/221

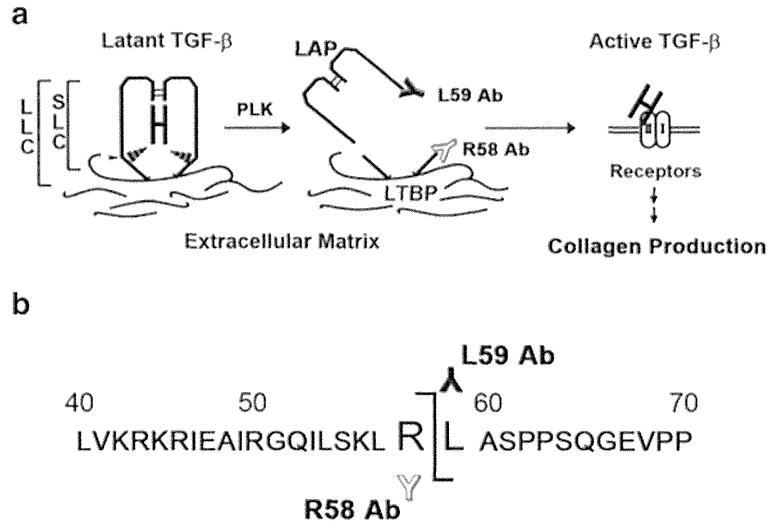

Figure 1 Determination of the LAP cleavage site produced during PLK-dependent TGF-β activation. (a) Schematic depiction of latent TGF-β1 activation by PLK. PLK cleaves LAP between R^{58} and L^{59} residues, which may destroy the interaction between LAP and active TGF-β1 molecule, releasing active TGF-β1 from the latent complex. LLC; large latent complex, SLC; small latent complex, LTBP; latent TGF-β binding protein. **(b)** The PLK cleavage site was determined by amino acid sequencing of LAP-DP isolated after SDS-PAGE. The amino acid sequences around the PLK cleavage site are illustrated. Antibodies (Ab), which specifically recognize cutting edges of LAP-DPs, were produced. White "Y" represents R58 antibody recognizing the N-terminal side R^{58} LAP-DP, whereas black "Y" represents L59 antibody recognizing the C-terminal side L^{59} LAP-DP.

TGF-β binding protein (LTBP), via C^{33} residues, forming the large latent complex (LLC). This complex can be sequestered in the ECM (Figure 1a) (Breitkopf et al. 2001). LTBP is a member of an ECM protein family, fibrillin (Zilberberg et al. 2012).

Several molecules are known to activate TGF-β1 in animal models. These include integrins (Nishimura 2009; Henderson et al. 2013), thrombospondin (Ribeiro et al. 1999), and proteases, such as matrix metalloproteinases (MMPs) (Yu and Stamenkovic 2000) and serine proteases (Jenkins 2008). Lyons R.M. *et al.* first reported that plasmin digests LAP and activates TGF-β1 *in vitro* (Lyons et al. 1990). Using a protease inhibitor, Camostat Mesilate, we previously demonstrated that plasma kallikrein (PLK) is involved in the TGF-β1 activation associated with liver fibrosis and impaired liver regeneration in animal models (Okuno et al. 2001; Akita et al. 2002). However, it remained to be elucidated whether PLK-dependent TGF-β1 activation also occurs during the pathogenesis of liver fibrosis in patients.

In this paper, we describe successful experiments aimed at generating specific antibodies against the two degradation products of LAP (LAP-DP) produced after PLK digestion, and the use of these antibodies to stain the LAP-DP in patient livers, thereby providing evidence of PLK-dependent TGF-β1 activation in human hepatic fibrosis. The results demonstrate the potential utility of the LAP-DP as a surrogate marker for PLK-dependent activation of TGF-β1 in the liver.

Results

Identification of LAP cleavage sites during proteolytic activation of latent TGF-β1

PLK primarily cleaved recombinant human LAP β1 (rhLAP β1) between R^{58} and L^{59} residues (Figure 1b). Further incubation resulted in cleavage between $R^{267}$and A^{268} residues.

Preparation of specific antibodies that recognize LAP neo-epitopes formed by PLK during TGF-β1 activation

Based on the amino acid sequences of PLK cleavage site, we prepared monoclonal antibodies that recognized the neo-epitopes formed within LAP during PLK-dependent TGF-β1 activation (Figure 1). The antibodies against the neo-C-terminal end of the PLK-cleaved N-terminal side LAP-DP ending at R^{58} (referred as R^{58} LAP-DP) and the neo-N-terminal end of the PLK-cleaved C-terminal side LAP-DP beginning from L^{59} (referred as L^{59} LAP-DP) were named R58 and L59 antibodies, respectively. Figure 2 shows Western blots using Glutathione-*S*-transferase (GST) fused-recombinant human latent TGF-β1 (GST-rhLTGF-β1) or rhLAP β1 (schematic structures are illustrated in panel a) to examine the specificities of R58 and L59 antibodies. The R58 antibody recognized only GST-fused R^{58} LAP-DP around 30 kD (panel b, lane 2), and the L59 antibody recognized the 29 kD of L^{59} LAP-DP (panel d, lane 2). However, both R58 and L59 antibodies did not recognize uncleaved GST-rhLTGF-β1 and rhLAP β1 (panels b and d, lane 1) that were detectable by the

Hara *et al. SpringerPlus* 2014, **3**:221
http://www.springerplus.com/content/3/1/221

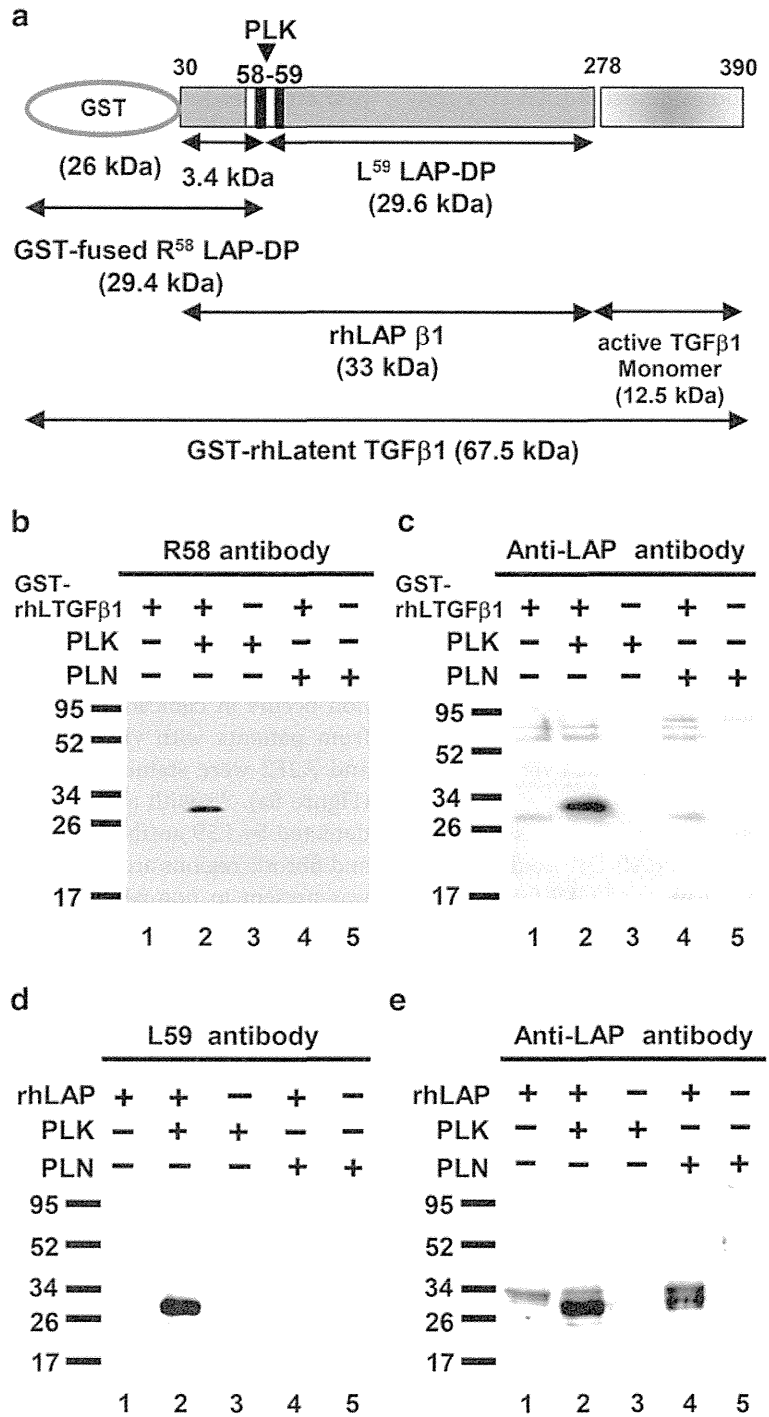

Figure 2 Specificity of R58 and L59 antibodies. (a) Schematic structure of a GST- rhLTGF-β1 protein generated in bacteria and a commercial rhLAP β1 generated in insect cells. The PLK cleavage site is indicated by arrowhead. **(b-e)** GST-LTGF-β1/rhLAP β1was incubated with/without PLK or PLN for 45 min at 37°C, and thereafter equal amounts of samples containing either 50 ng GST-rhLTGF-β1 or 500 ng rhLAP β1 were subjected to each lane in SDS-PAGE under reducing conditions followed by Western blot analyses using R58/L59 antibodies **(b, d, respectively)**. Membranes used in panels b and d were reprobed with monoclonal **(c)** or polyclonal **(e)** anti-LAP antibodies. *Lanes 1*, intact GST-rhLTGF-β1 or rhLAP-β1; *lanes 2*, PLK digested GST-rhLTGF-β1 or rhLAP-β1; *lanes 3*, PLK; *lane 4*, PLN digested GST-rhLTGF-β1 or rhLAP-β1; *lane 5*, PLN. Representative results from three independent experiments with a similar result are shown.

Hara et al. SpringerPlus 2014, 3:221
http://www.springerplus.com/content/3/1/221

monoclonal anti-LAP antibody recognizing N-terminal side LAP-DP (panel c) or the polyclonal anti-LAP antibody recognizing C-terminal side LAP-DP (panel e). Moreover, neither R58 nor L59 antibodies detected LAP-DPs generated by plasmin (PLN) digestion (panels b and d, lane 4) These data demonstrated that the anti-LAP antibodies recognize both LAP and PLK-cleaved LAP-DP, while the R58 and L59 antibodies specifically recognize only the respective LAP-DP. There are three isoforms of pro-TGF-βs. Amino acid sequences between E^{47} and L^{59} residues in LAP are identical between TGF-β1 and TGF-β3 (Additional file 1: Figure S1). Hence, we checked whether R58 antibody can recognize TGF-β3 LAP-DP as well as TGF-β1 LAP. As shown in Additional file 2: Figure S2, R58 antibody recognized PLK-digested TGF-β1 and β3 LAP peptide, but not non-digested and PLN-digested TGF-β1 and β3 LAP peptides (upper and lower lane, respectively) nor TGF-β2 LAP peptide, which does not have P1 site R^{58} residue, irrespective of PLK or PLN digestion (middle lane). These data suggested that R58 and L59 antibodies are promising tools to monitor cleavage of LAP by PLK, in other words, both R^{58} and L^{59} LAP-DPs can be footprints of PLK-dependent TGF-β1 as well as TGF-β3 activation.

Immunohistochemistry of murine fibrotic liver using R58 antibodies

Because LAP may be S-S bonded to LTBP present in the ECM, we expected that the R^{58} LAP-DP would remain within fibrotic tissues after cleavage of LAP by PLK. We tested this possibility in fibrotic livers from the carbon tetrachloride (CCl_4)-treated mice and bile duct ligated (BDL)-mice using R58 antibody. As shown in Figure 3, at 12 weeks after initiating CCl_4 treatment, CCl_4-treated mice displayed hepatocellular injury around the lobes (panel a) and bridging fibrosis from central veins to portal areas (panel b). The R^{58} LAP-DP was detectable and increased in CCl_4-treated mice (panel c), especially along fibrotic areas in CCl_4-treated mice compared with olive oil treated control mice. Positive area rates were increased 5-folds as written underneath panels c and f. Small positive spots seen in the control section were non-specific staining of mostly erythrocytes (panel f). Similar results were obtained from BDL mice (Figure 4). BDL mice often exhibited granulomatous lesions (panel a), in which fibroblastic cells infiltrated and started ECM production (panel b). The R^{58} LAP-DP was detected in granulomatous lesions prior to Sirius red positivity, namely before collagen accumulation (arrowheads in panel c). Positive areas were increased 3-folds as written underneath panels c and f. Signals from R^{58} LAP-DP was absorbed by pre-incubation of R58 antibody with antigen-peptides, and non-immune mouse IgG failed to yield a signal (Figure 5a-c), indicating that the signals were specific to R^{58} LAP-DP. We were unable to stain the L^{59} LAP-DP with L59 antibody although various antigen unmasking procedures were treated (Figure 5d). In, Figure 6, non-parenchymal regions were recognized by antibody R58 (red arrowheads in upper panels), and mostly overlapped with α-smooth muscle actin (αSMA)-positive activated hepatic stellate cells (HSCs) (red arrowheads in second row panels), but not with CD31-positive liver sinusoidal endothelial cells (third row panels) nor with F4/80-positive Kupffer cells (hepatic macrophages) (lower panels). Activated HSCs in the fibrotic liver were stained strongly with anti-pSmad3C antibody compared to olive oil-treated control mice (arrowheads in Figure 7, left panel), suggesting that TGF-β signaling was provoked. These data suggest that PLK-dependent TGF-β1/3 activation was induced in murine liver fibrosis models and that R^{58} LAP-DP, but not L^{59} LAP-DP, can be a footprint of the generation of active TGF-β1/3 in liver tissue.

Immunohistochemistry of fibrotic liver tissues from patients using R58 antibody

Finally, we evaluated human liver sections with the R58 antibody to determine if PLK-dependent TGF-β1/3 activation occurs in clinical liver diseases. Fibrotic liver tissues from patients with viral hepatitis categorized as A1F2 and A2F2 were stained robustly with the R58 antibody (Figure 8a). As with animal models, no signals could be detected by L59 antibody (Figure 8b). In peri-sinusoidal and fibrotic regions around the hepatic lobes, R^{58} LAP-DP was present in non-parenchymal cells, mainly in αSMA-positive HSC (arrows in Figure 8c). R58 signals could be detected along fibrous septa, implying that R^{58} LAP-DP accumulated within the ECM upon TGF-β1/3 activation. A similar staining with the R58 antibody was observed in patients with non-viral hepatitis, such as autoimmune hepatitis (AIH) and non-alcoholic steatohepatitis (NASH) (Figure 8d). These data clearly indicated that PLK-dependent TGF-β1/3 activation is induced during the pathogenesis of liver fibrosis in patients with a range of liver diseases, and that PLK-cleaved R^{58} LAP-DP might serve as a novel surrogate biomarker of TGF-β1/3 activation and its associated fibrosis in patients.

Discussion

An important step to control biological activity of TGF-β is its activation referred as "TGF-β activation." Proteolytic activation of latent TGF-β1 was first described in 1988 (Lyons et al. 1988) and was demonstrated in hepatic stellate cells during the pathogenesis of liver fibrosis and/or impaired liver regeneration in animal models (Okuno et al. 2001; Akita et al. 2002). Although we described PLK-dependent TGF-β activation in rodent models of the liver diseases, it remained to be elucidated whether this mechanism is also effective in patients.

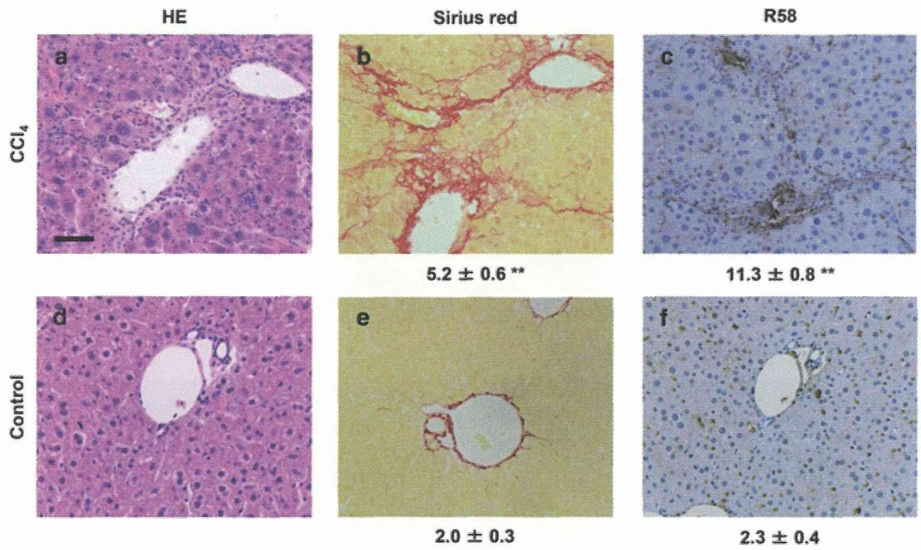

Figure 3 Immunohistochemistry of R^{58} LAP-DP in fibrotic liver tissues in CCl_4-treated mice using R58 antibody. Liver tissues from CCl_4-treated and control (olive oil administrated) mice were stained by HE **(a, d)** and Sirius Red **(b, e)**, and then immunostained with R58 antibody **(c, f)**. Scale bar = 50 μm. The percentage of fibrotic regions and R58 positive areas were calculated from three fields each from five sections (5 mice) (total 15 fields) and described as average ± SE under the corresponding panels. A total of 16 mice were evaluated and representative results are shown.

Here, we have identified PLK cleavage site within the LAP of latent TGF-β1, and have generated antibodies that specifically recognize the neo C- and N-termini of LAP-DPs (R58 and L59 antibodies, respectively) (Figure 1). These antibodies may be powerful tools to detect the footprints of latent TGF-β1 activation. Notably, we successfully used the antibodies to detect LAP-DP generated during TGF-β1 activation in human samples. For the first time, we demonstrated that the PLK-dependent activation of latent TGF-β1 is associated with human hepatic diseases with the use of the R58 antibody. This technique can be generally applied to measure activation of other cytokines, in which by-products corresponding to the LAP-DP are generated.

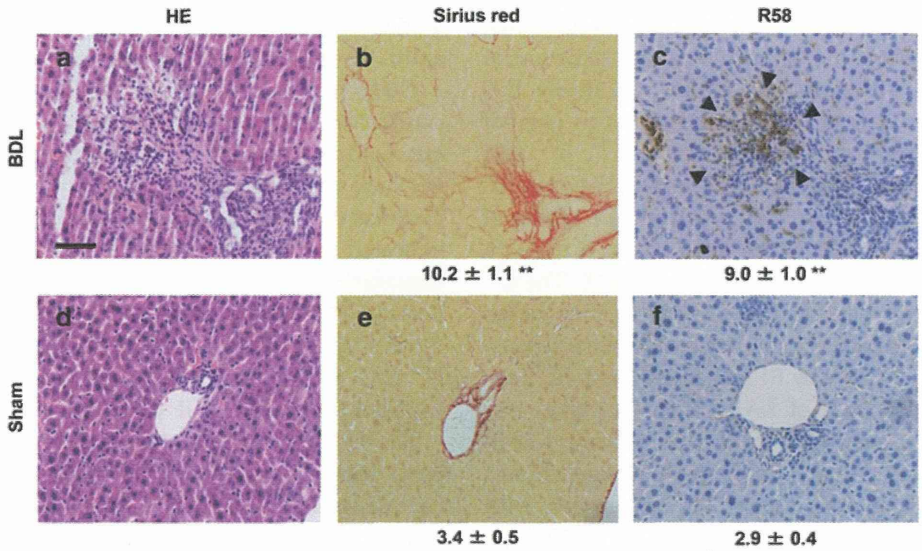

Figure 4 Immunohistochemistry of R^{58} LAP-DP in fibrotic liver tissues in BDL mice using R58 antibody. Liver tissues from BDL and sham-operated mice were stained by HE **(a, d)** and Sirius Red **(b, e)**, and then immunostained with R58 antibody **(c, f)**. Scale bar = 50 μm. The percentage of fibrotic regions and R58 positive areas were calculated from three fields each from five sections (5 mice) (total 15 fields) and described as average ± SE under the corresponding panels. A total of 16 mice were evaluated and representative results are shown.

Hara et al. SpringerPlus 2014, 3:221
http://www.springerplus.com/content/3/1/221

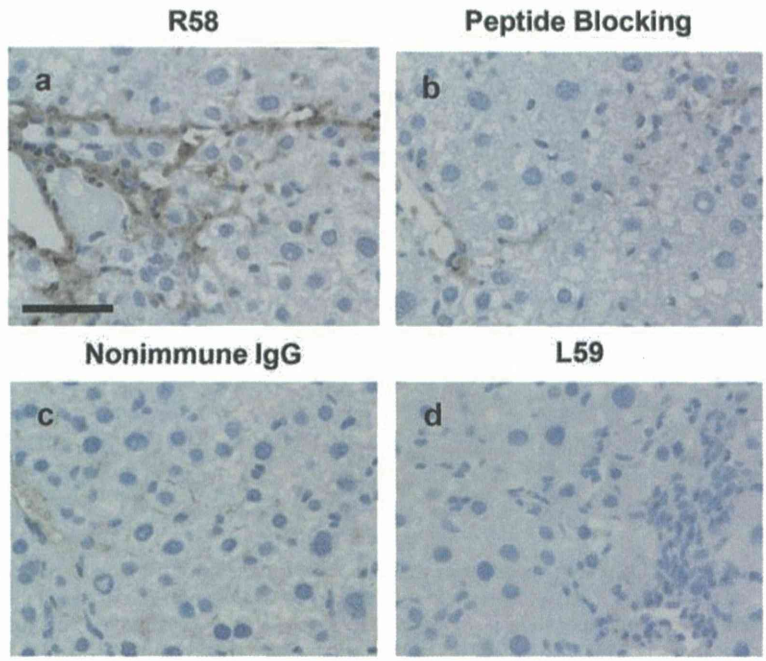

Figure 5 Control experiments for immunostaining with R58 and L59 antibodies. Serial liver sections of from CCl_4-treated mice at 12 weeks were stained with R58 antibody (1 μg/ml) **(a)**, R58 antibody (1 μg/ml) that had been pre-incubated with 10 μg/ml R58 antigen peptide **(b)**, the same concentration of nonimmune mouse IgG **(c)**, and L59 antibody (1 μg/ml) **(d)**. Scale bars = 25 μm. This picture shows the representative result from three independent experiments.

The primary cleavage site of LAP by PLK was between R^{58}-L^{59} (Figure 1b). Interestingly, the PLK cleavage site is proximal with the putative binding site for thrombospondin ($L^{54}SKL^{57}$) (Ribeiro et al. 1999). This suggests that the region containing $L^{54}SKLRL^{59}$ is important for maintaining TGF-β1 latency. Consistent with this idea, it was recently revealed that the active TGF-β1 molecule is associated with this region based both on mutational analysis (Walton et al. 2010) and the crystal structure of porcine latent TGF-β1 (Shi et al. 2011). Specifically, this sequence is located near the C-terminal end of α1 helix of LAP and hydrophobic residues containing L^{54}, L^{57}, and L^{59}, which are present along the inner face of the α1 helix, interact with W^{308}/W^{310} and with aliphatic side chains of active TGF-β1. The α1 helix is predicted to play a role of a 'straitjacket' for active TGF-β1 (Walton et al. 2010). The K^{56} fastens the *C*-terminal end of the α1 helix in cooperation with Y^{74}-A^{76}, and moreover associates S^{380} via hydrogen bonding (Shi et al. 2011). The P1 site amino acids (R^{58}) are located on the outer face of LAP, so PLK cleavage site should be highly accessible. Proteolytic cleavage within this region is likely to cause a conformational change of the LAP, resulting in a loss of its association with the active TGF-β1 molecule and release of active TGF-β1 molecule from the latent complex.

In Figure 2, we made monoclonal antibodies against both N- and C-terminal side LAP-DP (R^{58}/L^{59} LAP-DP) and checked their reaction specificities by western blotting. R58/L59 antibodies detected neither uncleaved LAP nor PLN-cleaved LAP-DP, and specifically recognized only PLK-cleaved LAP-DP, whereas anti-LAP antibodies recognized both uncleaved and PLK-cleaved LAP-DP. In Figure 2c, lane 4, we failed to detect N-terminal side LAP-DP made by PLN digestion with monoclonal anti-LAP antibody that nicely detected N-terminal side LAP-DP made by PLK digestion. We speculate that the epitope recognized by this anti-LAP antibody would be lost by PLN digestion.

Three isoforms of proTGF-β (β1-β3) have been characterized (Massague 1990), and LAP domains of different isoforms share 28-45% identity. TGF-β2 LAP does not have the sequences cleaved by PLK, whereas TGF-β3 LAP has the same sequences as TGF-β1 LAP. Our results indicated that PLK can cleave TGF-β3 LAP, and that their degradation products were detectable by R58 antibody. Because TGF-β3 expression is reported to be very weak in the liver (De Bleser et al. 1997), we think it is likely that the R^{58} LAP-DP we detected is derived mainly from TGF-β1 LAP, but partly from TGF-β3 LAP.

We also successfully detected PLK-cleaved R^{58} LAP-DP using the R58 antibody in fibrotic mice, suggesting that PLK dependent TGF-β1/3 activation was at least involved in murine hepatic fibrosis and that PLK-cleaved LAP-DP might be a marker for liver fibrosis. Our previous study demonstrated that PLN also plays an important role in liver fibrosis in the rat porcine serum model (Okuno et al. 2001), therefore we are now using the same strategy to produce

Hara *et al. SpringerPlus* 2014, **3**:221
http://www.springerplus.com/content/3/1/221

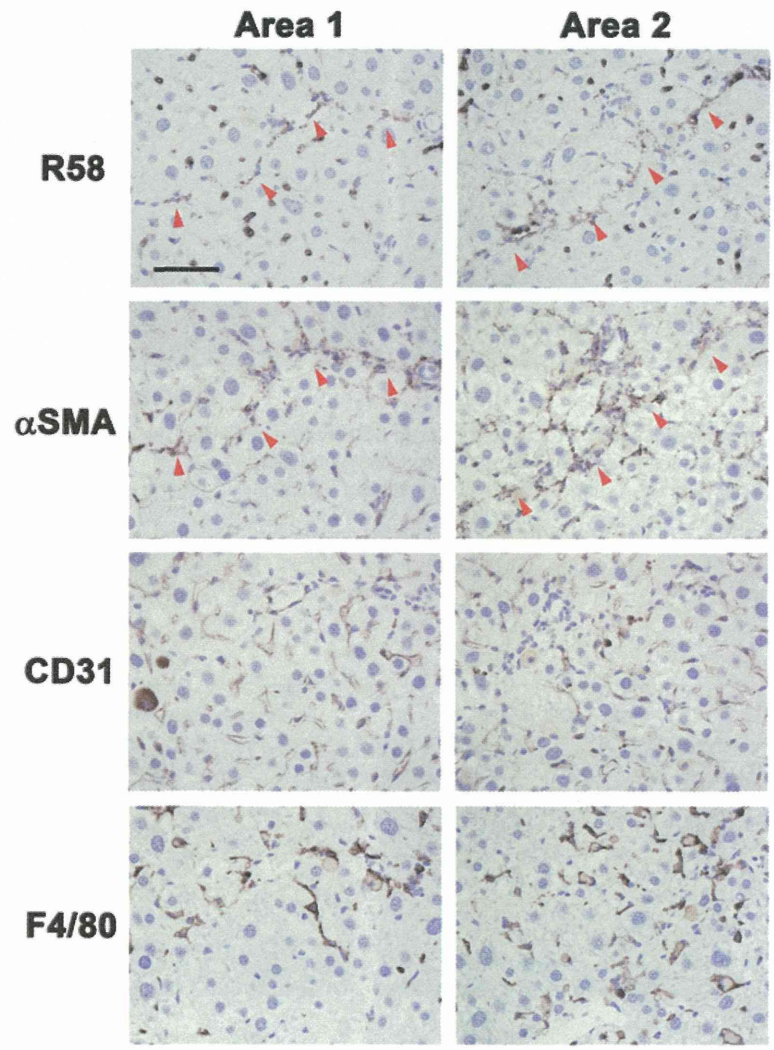

Figure 6 Identification of R58 positive cells in CCl_4-treated mice liver sections. Paraffin serial sections were immunostained with, R58 (upper panels), anti-αSMA (second row panels), anti-CD31 (third row panels), and anti-F4/80 (lower panels) antibodies. R58 positive signals were compared with αSMA, CD31, or F4/80 signals in same areas of each sections. The red arrowheads (R58 and αSMA panels) represent respectively both R58 and αSMA positive cells along with fibrotic septa. Scale bar = 50 μm.

antibodies that recognize PLN-cleaved LAP-DP. Similar to murine models, R^{58} LAP-DP was observed in patients suffering from hepatic diseases. Fibrous septa were obviously stained by the R58 antibody, indicating that R^{58} LAP-DP was generated at the site of the TGF-β1/3 activation and remained there. The intensity of R58 signals did not correlate with the severity of hepatic inflammation and fibrosis, so future studies will assess what drives increased R58 expression in vivo.

In contrast to the R58 antibody, we obtained essentially no positive signals with L59 antibody staining in both rodent and human samples. This suggests that C-terminal side L^{59} LAP-DP might be released after proteolytic digestion. Recently, we established an ELISA using the L59 antibody and successfully detected PLK-cleaved L^{59} LAP-DP generated in in vitro reactions. Currently, we are examining if we can detect L^{59} LAP-DP in plasma from animal models and patients, and if so, what is the clinical relevance of these values in liver diseases.

Integrins are known to activate TGF-β1, and it is reported that several subtypes of integrin, for example, $\alpha_v\beta6$, are related to hepatic fibrosis in both animal models and patients (Patsenker et al. 2008; Henderson and Sheppard 2013; Allison 2012). Because integrins, which are anchored to the cell membrane, stretch the LAP by interacting via the RGD motifs to release active TGF-β1, the LAP DP is not produced (Wipff et al. 2007). Therefore compared to integrins, PLK-cleaved R^{58} LAP-DP will serve as a more direct biomarker for TGF-β1 activation and following liver fibrosis.

Du X et al. showed that MMP-2 is related to renal fibrosis (Du et al. 2012). Several MMPs are also known to activate

Hara *et al. SpringerPlus* 2014, **3**:221
http://www.springerplus.com/content/3/1/221

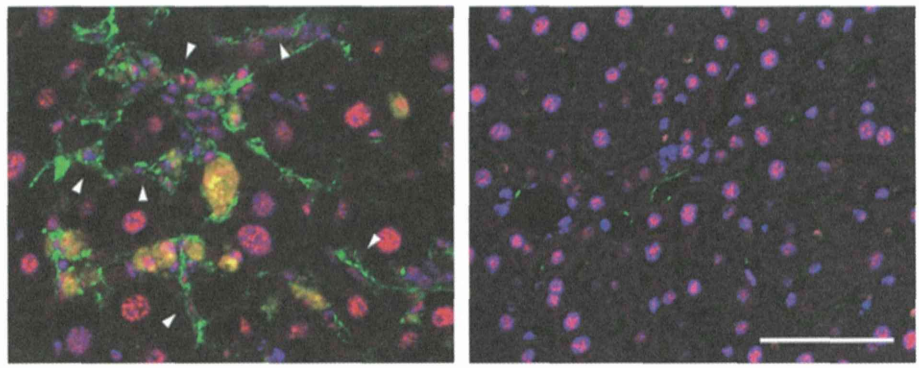

Figure 7 Detection of phosphorylated Smad3C in activated HSCs in CCl_4-treated mice liver sections. Phosphorylation and nuclear translocation of Smad3C in activated HSCs were examined by immunofluorescent double staining with anti-pSmad3C (red) and anti-αSMA (green) antibodies. Nuclei of the cells were identified by Hoechst 33258 staining (blue). The pSmad3C positive-activated HSCs were seen only in CCl_4-treated mice. Scale bar = 50 μm.

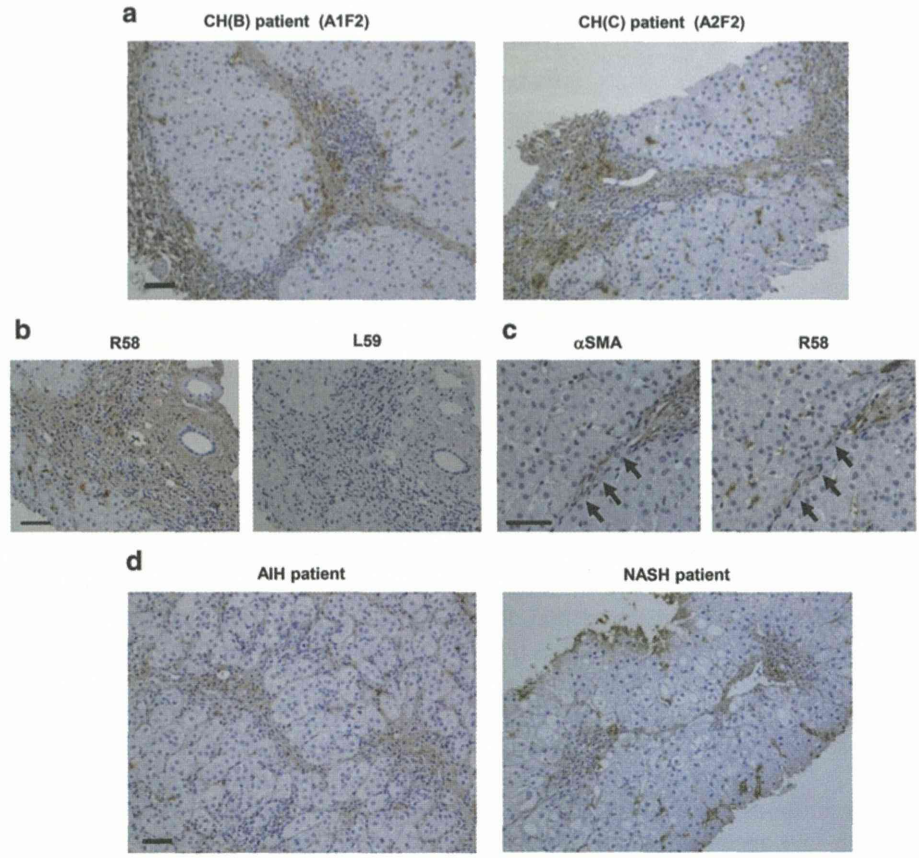

Figure 8 Immunostaining of biopsied human liver tissues. (a, d) Liver biopsy samples from four patients (chronic hepatitis B and C virus infection [CH (B) and (C), respectively], AIH with severe fibrosis, and NASH. The hepatitis activity grade and fibrosis score are described in the upper corresponding micrograms. **(b)** Serial sections from CH(C) patient were stained with R58 and L59 antibodies. **(c)** Liver specimens from another CH(B) patient were stained with anti-αSMA, R58 antibodies. αSMA and R58 signal positive cells lined up along fibrous septa (yellow arrows). Scale bars = 50 μm.

Hara *et al. SpringerPlus* 2014, **3**:221
http://www.springerplus.com/content/3/1/221

latent TGF-β1 (Yu and Stamenkovic 2000), although their cleavage sites within LAP have not been determined. Therefore, we are expanding our current method to detect MMP-mediated TGF-β1 activation in the kidney.

Conclusions

In summary, we demonstrate here 1) PLK cleaves LAP between R58 and L59 residues, 2) PLK-dependent TGF-β activation occurs in human hepatic fibrosis, and 3) PLK-cleaved LAP-DP is the potential surrogate marker for proteolytic TGF-β1/3 activation and in turn fibrogenesis in the liver.

Methods

Materials

Recombinant human TGF-β1 LAP (rhLAP β1) and both monoclonal and polyclonal anti-human LAP β1 antibodies (MAB246 and AF246, respectively) were purchased from R&D Systems (Minneapolis, MN). Human PLK was from CalBiochem (San Diego, CA). Anti-αSMA antibody were purchased from DAKO (Glostrup, DK). Anti-CD31 antibody was from dianova GmbH (Hamburg, DE). Anti-F4/80 antibody was from AbD serotec, LLC (Oxford, UK). Anti-pSmad3C polyclonal antibody was a kind gift from Dr. Matsuzaki (Kansai Med. Univ., Japan). GST-rhLTGF-β1 protein was prepared as described follows. A plasmid encoding GST-rhLTGF-β1 was constructed by inserting a human TGF-β1 cDNA into the pGEX-6P-1 vector (GE Healthcare, Buckinghamshire, UK), and protein expressed in *E. coli.* BL21 (Stratagene, La Jolla, CA) and purified using Glutathione Sepharose (GE Healthcare).

Determination of the cleavage sites within LAP by PLK

To identify the cleavage site in LAP during latent TGF-β1 activation by PLK, rhLAP β1 was incubated with PLK. After digestion, the resultant fragments were separated by SDS-polyacrylamide gel electrophoresis, and the N-terminal sequence of each LAP-DP was determined using a pulsed liquid protein sequencer Precise 494cLC (Hayashi et al. 2008).

Preparation of R58 and L59 monoclonal antibodies against neo C- and N-termini of LAP-DPs generated by PLK

Murine R58 and L59 monoclonal antibodies were generated against an 8 amino acid peptide, ending at R^{58} and plus a CG linker sequence at its N-terminus [CGGQILSKLR (Figure 1b)] and an 11 amino acid peptide, beginning from L^{59} and plus a GGC linker sequence [LASPPSQGEVPGGC (Figure 1b)]. BALB/c mice purchased from Charles River Laboratories Japan, Inc. (Kanagawa, Japan) were immunized with 50 μg of the antigen peptides. Once an appropriate titer had been achieved, fusion was performed using a protocol adapted from Lane *et al.* (Lane et al. 1986). Positive clones, which reacted to the BSA-conjugated antigen peptide, but not to the terminus-modified antigen peptide (the C-termini were amidated for R58 antibody, while the N termini were acetylated for L59 antibody production), were selected. The antibodies were purified through the Protein G column (GE Healthcare).

SDS-PAGE and Western blot analysis

GST-rhLTGF-β1 as well as rhLAP β1 were digested by co-incubation with PLK or PLK at 37°C for 45 min. Thereafter, equal amounts of samples containing either 50 ng of GST-rhLTGF-β1 or 500 ng of rhLAP β1 were subjected to each lane in SDS-PAGE under reducing conditions, followed by transfer onto PVDF membrane (Millipore, Bedford, MA). Western blot analyses were performed using either monoclonal R58 and L59 antibodies (2 μg/ml) plus HRP-conjugated anti-mouse antibodies (1:5,000) (Jackson Immuno Research Laboratories, Inc., West Grove, PA) and reprobed either with monoclonal or polyclonal anti-LAP antibodies. The bands were visualized by a Western Blotting Substrate Plus purchased from Thermo Scientific (Rockford, IL).

Animal models

Male C57BL/6 mice were purchased from Japan SLC Inc. (Shizuoka, Japan). All animals were maintained on a 12 hour light/12 hour dark cycle. Food and water were available *ad libitum.* All animal experiments were performed in accordance with protocols approved by the RIKEN Institutional Animal Use and Care Administrative Advisory Committee. For the CCl_4-induced liver fibrosis model, mice were injected intramuscularly with 50% CCl_4 (CCl_4: olive oil = 1:1, 2 ml/kg) twice a week for 12 weeks. Control animals were injected with the same volume of olive oil. Mice were sacrificed one week after the last CCl_4 injection. For the BDL model, ligation of the common bile duct was performed according to Arias *et al.* (Arias et al. 2003). Sham-operated mice were treated in the same manner except that the bile duct was not ligated. The animals were sacrificed at 14 days after operation.

Patient samples

The study was performed in accordance with the Declaration of Helsinki and was approved by the Ethics Committee for Biomedical Research of the Jikei University School of Medicine and RIKEN Institute Research Ethics Committee. All patients had signed a written informed consent prior to study. Liver biopsy samples were taken from patients suffering with cirrhotic liver diseases due to infection with types B and/or C hepatitis virus, AIH and NASH.

The stage of fibrosis and the grade of inflammatory activity were classified according to the METAVIR score (Bedossa and Poynard 1996).

Staining of liver tissue sections

Animal tissue specimens were fixed in 4% paraformaldehyde, and human biopsied samples were fixed in 10%

neutral buffered formalin. They were all embedded in paraffin. Sections (4 μm thickness) were stained by Hematoxylin and Eosin (HE), as well as 0.1% picro-sirius red solution for diagnostic purposes. For immunostaining of the LAP-DP, antigens were retrieved by microwave in citrate buffer (pH 6), and thereafter sections were incubated in 0.3% H_2O_2/methanol for 30 min to block endogenous peroxidases, followed by incubation in phosphate buffered saline with 0.1% Tween 20 (PBST) containing 5% skim milk for 30 min to prevent nonspecific binding. Serial sections were then incubated with R58 (1 μg/ml) or L59 (1 μg/ml) overnight at 4°C. As negative controls, slides were incubated with nonimmune IgG under the same conditions. EnVision/HRP (DAKO) was used as the second antibody. Serial sections were also immunostained with anti-αSMA (diluted with 1:100, an activated HSC marker), anti-CD31 (5 μg/ml, a liver sinusoidal endothelial cell marker), and anti-F4/80 (5 μg/ml, a Kupffer cell marker) antibodies. The sections were counterstained with Hematoxylin. Fibrosis was detected using Sirius red as previously described (Junqueira et al. 1979). Both fibrotic areas and R58 positive areas were measured in each of three fields of five independent sections by WinROOF image analysis software.

Immunofluorescent staining

Four μm of liver sections were deparaffinized and heated to 121°C in citrate buffer (pH6) by an autoclave for 10 min for antigen retrieval. After blocking with 3% BSA/10% normal goat serum/0.1 M glycine/PBST for 30 min, the sections were incubated with both anti-pSmad3C (2 μg/ml) and anti-αSMA (1:100) antibodies overnight at 4°C, followed by incubation with both Alexa Fluor 488 anti-rabbit IgG and Alexa Fluor 555 anti-mouse IgG (1:1000; red; Life Technologies, Carlsbad, CA) for 2 hours at room temperature. Thereafter, the sections were incubated with Hoechst 33258 (1:5000, DOJINDO Laboratories, Kumamoto, Japan) for 10 min at room temperature, and were mounted with Fluoromount (Diagnostic BioSystems, Pleasanton, CA). Image data were acquired on a Zeiss LSM 700 laser scanning confocal microscopy.

Statistical analysis

Quantitative data are shown as mean ± SE. The two-sample Wilcoxon rank-sum test was employed to evaluate difference between two groups. A p-value < 0.01 was considered as statistically significant.

Additional files

Additional file 1: Figure S1. Sequence alignment of three pro-TGF-β isoforms.

Additional file 2: Figure S2. Isoform specificity of R58 antibody.

Abbreviations

LAP: Latency-associated protein; TGF-β: Transforming growth factor-β; ECM: Extracellular matrix; SLC: Small latent complex; LTBP: Latent TGF-β binding protein; LLC: Large latent complex; MMP: Matrix metalloproteinase; PLK: Plasma kallikrein; LAP-DP: Degradation product of LAP; rhLAP β1: Recombinant human LAP β1; R^{58} LAP-DP: PLK-cleaved N-terminal side LAP-DP ending at R^{58}; L^{59} LAP-DP: PLK-cleaved C-terminal side LAP-DP beginning from L59; GST: Glutathione-S-transferase; PLN: Plasmin; CCl_4: Carbon tetrachloride; BDL: Bile duct ligation; αSMA: α-smooth muscle actin; HSC: Hepatic stellate cell; AIH: Autoimmune hepatitis; NASH: Non-alcoholic steatohepatitis; HE: Hematoxylin and Eosin; PBST: Phosphate buffered saline with 0.1% Tween 20.

Competing interests

The authors declare that they have no competing interests. Although Shinji Ogawa is an employee of Pfizer Inc., this did not affect the experimental design or interpretation of the results.

Authors' contributions

HM and KA performed experiments. HM also wrote the manuscript. KW, OS, and IOS contributed to the production of the antibodies. MT and NK collected biopsied human liver samples and discussed the staining data. DN performed the protein sequences for determination of PLK cleavage sites within LAP. FSL, RDB, and KS planned the research. KS supervised the entire project. All authors read and approved the final manuscript.

Acknowledgments

We thank Dr. Matsuzaki (Kansai Medical University) for providing phospho-Smad3C antibodies. This work was supported partly by the Program for Promotion of Fundamental Studies in Health Science of National Institute of Biomedical Innovation (NIBL) and a grant from the "Chemical Genomics Research program" from RIKEN (to S.K.), the Uehara Memorial Foundation, Japan (to S.K.), the Research on the Innovative Development and the Practical Application of New Drugs for Hepatitis B (Principal investigator: Soichi Kojima; H24-B Drug Discovery-Hepatitis-General-003) provided by the Ministry of Health, Labor and Welfare of Japan, from the NIDDK, RO1DK56621 (to S.L.F.) and NCI, RO1 CA03482 and NIAMS, PPG AR049698 (to D.B.R.).

Author details

[1]Micro-signaling Regulation Technology Unit, RIKEN Center for Life Science Technologies, 2-1 Hirosawa, Wako, Saitama 351-0918, Japan. [2]Department of Laboratory Medicine, The Jikei University School of Medicine, Minato-ku, Tokyo 105-0003, Japan. [3]Division of Gastroenterology and Hepatology, Department of Internal Medicine, The Jikei University School of Medicine, Minato-ku, Tokyo 105-0003, Japan. [4]Biomolecular Characterization Team, Chemical Biology Core Facility, Chemical Biology Department, RIKEN Advanced Science Institute, Wako, Saitama 351-0918, Japan. [5]St. Louis Laboratories, Pfizer Worldwide Research & Development, Chesterfield, MO 63166, U.S.A. [6]Institute of Medical Science, University of Tokyo, Minato-ku, Tokyo 108-8639, Japan. [7]Division of Liver Diseases, Icahn School of Medicine at Mount Sinai, New York, NY 10029, U.S.A. [8]Department of Cell Biology, New York University School of Medicine, New York, NY 10016, U.S.A.

Received: 17 December 2013 Accepted: 8 April 2014
Published: 1 May 2014

References

Akita K, Okuno M, Enya M, Imai S, Moriwaki H, Kawada N, Suzuki Y, Kojima S (2002) Impaired liver regeneration in mice by lipopolysaccharide via TNF-alpha/kallikrein-mediated activation of latent TGF-beta. Gastroenterology 123(1):352–364

Allison M (2012) Stromedix acquisition signals growing interest in fibrosis. Nat Biotechnol 30(5):375–376. doi:10.1038/nbt0512-375

Arias M, Sauer-Lehnen S, Treptau J, Janoschek N, Theuerkauf I, Buettner R, Gressner AM, Weiskirchen R (2003) Adenoviral expression of a transforming growth factor-beta1 antisense mRNA is effective in preventing liver fibrosis in bile-duct ligated rats. BMC Gastroenterol 3:29. doi:10.1186/1471-230X-3-29

Bataller R, Brenner DA (2005) Liver fibrosis. J Clin Invest 115(2):209–218. doi:10.1172/JCI24282

Bedossa P, Poynard T (1996) An algorithm for the grading of activity in chronic hepatitis C. The METAVIR Cooperative Study Group. Hepatology 24(2):289–293. doi:10.1002/hep.510240201

Breitkopf K, Lahme B, Tag CG, Gressner AM (2001) Expression and matrix deposition of latent transforming growth factor beta binding proteins in normal and fibrotic rat liver and transdifferentiating hepatic stellate cells in culture. Hepatology 33(2):387–396. doi:10.1053/jhep.2001.21996

Dabovic B, Rifkin DB (2008) TGF-β Bioavailability: Latency, Targeting, and Activation. In: Derynck R, Miyazono K (ed) The TGF-β Family. Cold Spring Harbor Laboratory Press, Cold Spring Harbor, NY, pp 179–202

De Bleser PJ, Niki T, Rogiers V, Geerts A (1997) Transforming growth factor-beta gene expression in normal and fibrotic rat liver. J Hepatol 26(4):886–893

Dooley S, ten Dijke P (2012) TGF-beta in progression of liver disease. Cell Tissue Res 347(1):245–256. doi:10.1007/s00441-011-1246-y

Du X, Shimizu A, Masuda Y, Kuwahara N, Arai T, Kataoka M, Uchiyama M, Kaneko T, Akimoto T, Iino Y, Fukuda Y (2012) Involvement of matrix metalloproteinase-2 in the development of renal interstitial fibrosis in mouse obstructive nephropathy. Lab Invest 92(8):1149–1160. doi:10.1038/labinvest.2012.68

Hayashi M, Tamura Y, Dohmae N, Kojima S, Shimonaka M (2008) Plasminogen N-terminal activation peptide modulates the activity of angiostatin-related peptides on endothelial cell proliferation and migration. Biochem Biophys Res Commun 369(2):635–640. doi:10.1016/j.bbrc.2008.02.050

Henderson NC, Sheppard D (2013) Integrin-mediated regulation of TGFbeta in fibrosis. Biochim Biophys Acta 1832(7):891–896. doi:10.1016/j.bbadis.2012.10.005

Henderson NC, Arnold TD, Katamura Y, Giacomini MM, Rodriguez JD, McCarty JH, Pellicoro A, Raschperger E, Betsholtz C, Ruminski PG, Griggs DW, Prinsen MJ, Maher JJ, Iredale JP, Lacy-Hulbert A, Adams RH, Sheppard D (2013) Targeting of alphav integrin identifies a core molecular pathway that regulates fibrosis in several organs. Nat Med 19(12):1617–1624. doi:10.1038/nm.3282

Jenkins G (2008) The role of proteases in transforming growth factor-beta activation. Int J Biochem Cell Biol 40(6–7):1068–1078. doi:10.1016/j.biocel.2007.11.026

Junqueira LC, Bignolas G, Brentani RR (1979) Picrosirius staining plus polarization microscopy, a specific method for collagen detection in tissue sections. Histochem J 11(4):447–455

Lane RD, Crissman RS, Ginn S (1986) High efficiency fusion procedure for producing monoclonal antibodies against weak immunogens. Methods Enzymol 121:183–192

Lyons RM, Keski-Oja J, Moses HL (1988) Proteolytic activation of latent transforming growth factor-beta from fibroblast-conditioned medium. J Cell Biol 106(5):1659–1665

Lyons RM, Gentry LE, Purchio AF, Moses HL (1990) Mechanism of activation of latent recombinant transforming growth factor beta 1 by plasmin. J Cell Biol 110(4):1361–1367

Massague J (1990) The transforming growth factor-beta family. Annu Rev Cell Biol 6:597–641. doi:10.1146/annurev.cb.06.110190.003121

Nishimura SL (2009) Integrin-mediated transforming growth factor-beta activation, a potential therapeutic target in fibrogenic disorders. Am J Pathol 175(4):1362–1370. doi:10.2353/ajpath.2009.090393

Okuno M, Akita K, Moriwaki H, Kawada N, Ikeda K, Kaneda K, Suzuki Y, Kojima S (2001) Prevention of rat hepatic fibrosis by the protease inhibitor, camostat mesilate, via reduced generation of active TGF-beta. Gastroenterology 120(7):1784–1800

Patsenker E, Popov Y, Stickel F, Jonczyk A, Goodman SL, Schuppan D (2008) Inhibition of integrin alphavbeta6 on cholangiocytes blocks transforming growth factor-beta activation and retards biliary fibrosis progression. Gastroenterology 135(2):660–670. doi:10.1053/j.gastro.2008.04.009

Ribeiro SM, Poczatek M, Schultz-Cherry S, Villain M, Murphy-Ullrich JE (1999) The activation sequence of thrombospondin-1 interacts with the latency-associated peptide to regulate activation of latent transforming growth factor-beta. J Biol Chem 274(19):13586–13593

Shi M, Zhu J, Wang R, Chen X, Mi L, Walz T, Springer TA (2011) Latent TGF-beta structure and activation. Nature 474(7351):343–349. doi:10.1038/nature10152

Walton KL, Makanji Y, Chen J, Wilce MC, Chan KL, Robertson DM, Harrison CA (2010) Two distinct regions of latency-associated peptide coordinate stability of the latent transforming growth factor-beta1 complex. J Biol Chem 285 (22):17029–17037. doi:10.1074/jbc.M110.110288

Wipff PJ, Rifkin DB, Meister JJ, Hinz B (2007) Myofibroblast contraction activates latent TGF-beta1 from the extracellular matrix. J Cell Biol 179(6):1311–1323. doi:10.1083/jcb.200704042

Yu Q, Stamenkovic I (2000) Cell surface-localized matrix metalloproteinase-9 proteolytically activates TGF-beta and promotes tumor invasion and angiogenesis. Genes Dev 14(2):163–176

Zilberberg L, Todorovic V, Dabovic B, Horiguchi M, Courousse T, Sakai LY, Rifkin DB (2012) Specificity of latent TGF-beta binding protein (LTBP) incorporation into matrix: role of fibrillins and fibronectin. J Cell Physiol 227(12):3828–3836. doi:10.1002/jcp.24094

doi:10.1186/2193-1801-3-221
Cite this article as: Hara *et al.*: LAP degradation product reflects plasma kallikrein-dependent TGF-β activation in patients with hepatic fibrosis. *SpringerPlus* 2014 **3**:221.

Am J Physiol Gastrointest Liver Physiol 304: G293–G299, 2013.
First published October 18, 2012; doi:10.1152/ajpgi.00083.2012.

Innate immune responses involving natural killer and natural killer T cells promote liver regeneration after partial hepatectomy in mice

Satoko Hosoya,[1] Kenichi Ikejima,[1] Kazuyoshi Takeda,[2] Kumiko Arai,[1] Sachiko Ishikawa,[1] Hisafumi Yamagata,[1] Tomonori Aoyama,[1] Kazuyoshi Kon,[1] Shunhei Yamashina,[1] and Sumio Watanabe[1]

[1]*Department of Gastroenterology, Juntendo University Graduate School of Medicine, Tokyo, Japan; and* [2]*Department of Immunology, Juntendo University Graduate School of Medicine, Tokyo, Japan*

Submitted 29 February 2012; accepted in final form 7 October 2012

Hosoya S, Ikejima K, Takeda K, Arai K, Ishikawa S, Yamagata H, Aoyama T, Kon K, Yamashina S, Watanabe S. Innate immune responses involving natural killer and natural killer T cells promote liver regeneration after partial hepatectomy in mice. *Am J Physiol Gastrointest Liver Physiol* 304: G293–G299, 2013. First published October 18, 2012; doi:10.1152/ajpgi.00083.2012.—To clarify the roles of innate immune cells in liver regeneration, here, we investigated the alteration in regenerative responses after partial hepatectomy (PH) under selective depletion of natural killer (NK) and/or NKT cells. Male, wild-type (WT; C57Bl/6), and CD1d-knockout (KO) mice were injected with anti-NK1.1 or anti-asialo ganglio-*N*-tetraosylceramide (GM1) antibody and then underwent the 70% PH. Regenerative responses after PH were evaluated, and hepatic expression levels of cytokines and growth factors were measured by real-time RT-PCR and ELISA. Phosphorylation of STAT3 was detected by Western blotting. Depletion of both NK and NKT cells with an anti-NK1.1 antibody in WT mice caused drastic decreases in bromodeoxyuridine uptake, expression of proliferating cell nuclear antigen, and cyclin D1, 48 h after PH. In mice given NK1.1 antibody, increases in hepatic TNF-α, IL-6/phospho-STAT3, and hepatocyte growth factor (HGF) levels following PH were also blunted significantly, whereas IFN-γ mRNA levels were not different. CD1d-KO mice per se showed normal liver regeneration; however, pretreatment with an antiasialo GM1 antibody to CD1d-KO mice, resulting in depletion of both NK and NKT cells, also blunted regenerative responses. Collectively, these observations clearly indicated that depletion of both NK and NKT cells by two different ways results in impaired liver regeneration. NK and NKT cells most likely upregulate TNF-α, IL-6/STAT3, and HGF in a coordinate fashion, thus promoting normal regenerative responses in the liver.

innate immunity; TNF-α; IL-6; STAT3; hepatocyte growth factor

LINES OF EVIDENCE HAVE SUGGESTED that alteration in the innate immune system is involved in a variety of pathophysiological conditions in the liver (24). It is well known that the liver contains a variety of immune cells, with a considerable proportion of natural killer (NK) and NKT cell fractions (6). NK cells are defined as large, granular lymphocytes that exert cytotoxic activity against tumors and viral-infected cells through the perforin and granzyme systems (27). NK cells preferentially reside in the hepatic sinusoid, and these liver-specific NK cells are called Pit cells (31). On the other hand, NKT cells are a heterogeneous subset of lymphocytes expressing both NK and T cell surface markers (8, 14). NKT cells recognize a glycolipid antigen presented by CD1d, one of the major histocompatibility complex molecules, on antigen-presenting cells, such as dendritic cells and macrophages (3, 8). Several studies suggested that NKT cells modulate hepatic inflammation and fibrogenesis (7, 12, 21, 23, 25); however, the precise role of these cells in liver pathophysiology is still controversial.

Liver regeneration is one of the significant natures of this important organ. The normal liver is capable of regenerating when injured by various pathogens and mechanical damages (20, 29). The mechanism underlying this process has been studied from various aspects; however, it still remains unclear. Recent lines of evidence indicated that innate immune responses play a key role in the trigger and promotion of the regenerating process (5). For example, pattern-recognition receptors, such as Toll-like receptors, and downstream signaling involved in production of cytokines from hepatic macrophages (Kupffer cells) are quite important in liver regeneration (11, 26). However, the role of other types of innate immune cells, such as NK and NKT cells, in liver regeneration has not been fully elucidated. A recent report indicated that NK cells negatively regulate liver regeneration through production of IFN-γ (28). The role of NKT cells in liver regeneration is more obscure; poor regeneration in steatotic liver in ob/ob mice has been reported (16, 32), where hepatic NKT cells are depleted (17). Similarly, we have shown recently that KK-A^y mice, which develop a metabolic, syndrome-like phenotype spontaneously, demonstrate poor regeneration following 70% partial hepatectomy (PH) (2), where hepatic NKT cells are also depleted. Furthermore, activation of NKT cells triggered by a specific ligand α-galactosylceramide has been shown to accelerate liver regeneration after PH (22). These observations suggested that NKT cells promote the regeneration process; however, mice lacking NKT cells caused by genetic knockout (KO) of CD1d have been shown to demonstrate almost normal liver regeneration after PH (28).

In the present study, we therefore investigated the role of hepatic NK and NKT cells in liver regeneration following PH using mice lacking NK and/or NKT cells generated by a combination of KO animals and selective depletion of these cells by specific antibodies.

MATERIALS AND METHODS

Animal experiments. Male, wild-type (WT) C57Bl/6 mice, 7 wk after birth, were obtained from CLEA Japan (Tokyo, Japan). A colony of CD1d-KO mice raised from the C57Bl/6 strain (a generous gift from the Department of Immunology, Juntendo University of Medicine, Tokyo, Japan) was maintained in the animal facility in our institution—Juntendo University Graduate School of Medicine (9, 19). All animals received humane care in compliance with the experimental protocol approved by the Committee of Laboratory Animals, according to institutional guidelines. Mice were housed in air-condi-

Address for reprint requests and other correspondence: K. Ikejima, Dept. of Gastroenterology, Juntendo Univ. Graduate School of Medicine, 2-1-1 Hongo, Bunkyo-ku, Tokyo, 113-8421 Japan (e-mail: ikejima@juntendo.ac.jp).

tioned, specific pathogen-free animal quarters with lighting from 0800 to 2000 and were given unrestricted access to standard lab chow and water for 1 wk prior to experiments. After overnight fasting, 70% PH was performed in the mice, according to the Higgins and Anderson method (10). Some mice were given a single intraperitoneal injection of a mouse anti-NK1.1 MAb (PK136; 150 μg/body; provided by the Department of Immunology, Juntendo University School of Medicine) or an anti-asialo ganglio-*N*-tetraosylceramide (GM1) antibody (200 μg/body; provided by the Department of Immunology, Juntendo University School of Medicine), 24 h prior to operation. For the extended time course over 72 h following PH, mice were given the second injection of antibodies at 48 h after PH. Mice were killed by exsanguination from inferior vena cava, and serum and liver samples were obtained. Some mice were pulse labeled with a single intraperitoneal injection of bromodeoxyuridine (BrdU; Sigma Chemical, St. Louis, MO; 50 mg/kg in PBS), 2 h prior to death, and liver specimens were fixed in buffered formalin for immunohistochemistry. Serum and liver samples were kept frozen at −80°C until assayed.

Immunohistochemistry. For immunohistochemistry, formalin-fixed and paraffin-embedded tissue sections were deparaffinized and incubated with 3% H_2O_2 for 10 min. To examine BrdU incorporation to hepatocyte nuclei, tissue sections were incubated with 2 N HCl for 30 min. After blocking with normal horse serum for 60 min, tissue sections were incubated with a mouse anti-BrdU MAb (DakoCytomation Norden A/S, Glostrup, Denmark). After rinsing the primary antibody, the sections were incubated with secondary biotinylated antimouse IgG antibody, and specific binding was visualized with avidin-biotin complex solution, followed by incubation with a 3,3-diaminobenzidine tetrahydrochloride solution using the Vectastain Elite ABC kit (Vector Laboratories, Burlingame, CA). BrdU-positive hepatocytes were counted in five 100× fields on each slide to determine the average number BrdU-labeling index (BrdU-positive hepatocytes/total hepatocytes). Expression of proliferating cell nuclear antigen (PCNA) in hepatocytes was evaluated similarly by immunohistochemistry as described previously elsewhere (1). Specimens were observed and photographed using a microscope equipped with a digital imaging system (Leica DM 2000; Leica Microsystems GmbH, Germany).

Western blot analysis. Whole liver protein extracts were prepared by homogenizing frozen tissue in a buffer containing 50 mM Tris-HCl (pH 8.0), 150 mM NaCl, 1 mM EDTA, 1% Triton X-100, protease inhibitors (cOmplete, mini protease inhibitor cocktail tablets; Roche Diagnostics, Mannheim, Germany), and a phosphatase inhibitor Na_3VO_4 (50 μM; Sigma Chemical), followed by centrifugation at 15,000 rpm for 10 min. Protein concentration was determined by Bradford assay using the Bio-Rad protein assay kit (Bio-Rad Laboratories, Hercules, CA). Twenty micrograms of protein was separated in 10% SDS-PAGE and electrophoretically transferred onto polyvinylamide fluoride membranes. After blocking with 5% nonfat dry milk in Tris-buffered saline, membranes were incubated overnight at 4°C with rabbit polyclonal anticyclin D1 or antiphospho-STAT3 (Tyr705; Cell Signaling Technology, Beverly, MA), followed by a secondary horseradish peroxidase-conjugated antirabbit IgG antibody (DakoCytomation Norden A/S). Subsequently, specific bands were visualized using the enhanced chemiluminescence detection kit (GE Healthcare, Buckinghamshire, UK). Images were captured using a lumino-image analyzer (LAS-3000; Fujifilm, Tokyo, Japan), and densitometry was performed using Multi Gauge software (Fujifilm).

ELISA. Hepatocyte growth factor (HGF) levels in the liver homogenate were determined using an ELISA kit (Institute of Immunology, Tokyo, Japan), according to the manufacturer's instruction. Serum IL-6 levels were measured similarly by an ELISA kit (R&D Systems, Minneapolis, MN).

Cell culture. Hepatic stellate cell (HSC)-T6 cells, a rat HSC line, were cultured on polystyrene dishes using DMEM (Invitrogen, Carlsbad, CA), supplemented with 10% FBS in a humidified air containing 5% CO_2 at 37°C. Cells were then incubated with recombinant murine IFN-γ, TNF-α, IL-4, or IL-13 (10 ng/ml each; R&D Systems) for 3–6 h as appropriate.

RNA preparation and real-time RT-PCR. Total RNA was prepared from frozen tissue samples or culture cells using the illustra RNAspin Mini RNA Isolation kit (GE Healthcare). The concentration and purity of isolated RNA were determined by measuring optical density at 260 and 280 nm. Furthermore, the integrity of RNA was verified by electrophoresis on formaldehyde-denaturing agarose gels.

For real-time RT-PCR, total RNA (1 μg) was reverse transcribed using Moloney murine leukemia virus transcriptase (SuperScript II, Invitrogen) and an oligo(dT) 12–18 primer (Invitrogen) at 42°C for 1 h. Obtained cDNA (1 μg) was amplified using SYBR Premix Ex Taq (Takara Bio, Tokyo, Japan) and specific primers for IFN-γ, TNF-α, HGF, IL-4, IL-6, suppressor of cytokine signal (SOCS)-3, and GAPDH, as appropriate (Table 1). After a 10-s activation period at 95°C, 40 cycles of 95°C for 5 s and 60°C for 31 s, followed by the final cycle of 95°C for 15 s, 60°C for 1 min, and 95°C for 15 s, were performed using the ABI PRISM 7700 sequence detection system (PE Applied Biosystems, Foster City, CA), and the threshold cycle values were obtained.

Statistical analysis. Data were expressed as means ± SE. Statistical differences between means were determined using two-way ANOVA or ANOVA on ranks, followed by a post hoc test (Student-Newman-Keuls all pairwise comparison procedures) as appropriate. A value of $P < 0.05$ was selected before the study to reflect significance.

Table 1. *Primer sets for real-time RT-PCR*

Gene (GeneBank Accession)	Primer Sequences	Product Size
IFN-γ (NM_008337.3)	forward: 5′-CGGCACAGTCATTGAAAGCCTA-3′ reverse: 5′-GTTGCTGATGGCCTGATTGTC-3′	199 bp
TNF-α (NM_013693.2)	forward: 5′-AAGCCTGTAGCCCACGTCGTA-3′ reverse: 5′-GGCACCACTAGTTGGTTGTCTTTG-3′	122 bp
HGF (NM_010427.4)	forward: 5′-AGAAATGCAGTCAGCACCATCAAG-3′ reverse: 5′-GATGGCACATCCACGACCAG-3′	179 bp
IL-4 (NM_021283.2)	forward: 5′-ACGGAGATGGATGTGCCAAAC-3′ reverse: 5′-AGCACCTTGGAAGCCCTACAGA-3′	83 bp
IL-6 (NM_031168.1)	forward: 5′-CCACTTCACAAGTCGGAGGCTTA-3′ reverse: 5′-GCAAGTGCATCATCGTTGTTCATAC-3′	112 bp
SOCS-3 (NM_007707)	forward: 5′-CAATACCTTTGACAAGCGGACTCTC-3′ reverse: 5′-TCAAAGCGCAAACAAGTTCCAG-3′	146 bp
GAPDH (NM_008084.2)	forward: 5′-TGTGTCCGTCGTGGATCTGA-3′ reverse: 5′-TTGCTGTTGAAGTCGCAGGAG-3′	150 bp

HGF, hepatocyte growth factor; SOCS-3, suppressor of cytokine signal-3.